

See discussions, stats, and author profiles for this publication at: <https://www.researchgate.net/publication/239161479>

# Theoretical and crystallographic study of edge-to-face aromatic interactions between pyridine moieties and benzene

ARTICLE *in* CHEMICAL PHYSICS LETTERS · JANUARY 2009

Impact Factor: 1.9 · DOI: 10.1016/j.cplett.2008.12.007

CITATIONS

13

READS

21

## 5 AUTHORS, INCLUDING:



**Daniel Escudero**

University of Nantes

50 PUBLICATIONS 1,118 CITATIONS

SEE PROFILE



**Antonio Frontera**

University of the Balearic Islands

276 PUBLICATIONS 5,595 CITATIONS

SEE PROFILE



**David Quiñonero**

University of the Balearic Islands

139 PUBLICATIONS 4,152 CITATIONS

SEE PROFILE



**Pere M Deyà**

University of the Balearic Islands

172 PUBLICATIONS 4,660 CITATIONS

SEE PROFILE



# Theoretical and crystallographic study of edge-to-face aromatic interactions between pyridine moieties and benzene

Daniel Escudero, Carolina Estarellas, Antonio Frontera<sup>\*</sup>, David Quiñonero, Pere M. Deyà<sup>\*</sup>

Departament de Química, Universitat de les Illes Balears, 07122 Palma de Mallorca, Spain

## ARTICLE INFO

### Article history:

Received 6 November 2008

In final form 1 December 2008

Available online 7 December 2008

## ABSTRACT

The T-shaped aromatic non-covalent interaction involving pyridine and benzene rings is studied by means of RI-MP2/aug-cc-pVTZ *ab initio* calculations. They indicate that the participation of the nitrogen atom of pyridine in a variety of interactions or bonding (coordinated to a metal, hydrogen bonding, N-oxide derivative or protonation) affects the edge-to-face aromatic interaction with benzene. This long distance effect has been studied using the 'atoms-in-molecules' theory and the Molecular Interaction Potential with polarization (MIPp) partition scheme. Experimental evidence for such interactions has been obtained from the Cambridge Structural Database.

© 2008 Elsevier B.V. All rights reserved.

## 1. Introduction

Non-covalent interactions involving aromatic rings are key processes in both chemical and biological recognition [1], since supramolecular chemistry rely on these forces. Interactions between aromatic rings ( $\pi$ – $\pi$  interactions) contribute to protein and DNA stability [2–4] and form recognition motifs in proteins and enzymes [5,6]. Several studies suggest the existence of a competition between stacking and T-shaped (edge-to-face) complexes involving aromatic amino acids. This competition [7,8] is strongly affected by the polarity of the environment and by the possibility of forming hydrogen bonds [9]. The latter point is still under discussion since recent studies have shown that (i) the favourable nature of stacked conformations in protein environment must not be related with the higher accessibility of H-bond forming groups [10] and (ii) that the  $\pi$ – $\pi$  interaction on itself does not have an overall strengthening on hydrogen bonding in DNA [11].

The  $\pi$ – $\pi$  interaction is dominated by dispersion and electrostatic (quadrupole–quadrupole) forces. The T-shaped orientation has favourable electrostatics but weaker dispersion and it is very close in energy to the parallel displaced configuration that has more dispersion but less favourable electrostatics. High accuracy benchmark calculations on the benzene dimer demonstrate that both configurations have a binding energy of 2.5 kcal/mol [12,13]. This result is in line with the competition between stacking and T-shaped configurations in aromatic interactions in amino acids [7].

We have recently reported experimental [14] and theoretical [15,16] evidence of interesting synergistic effects between a

variety of non-covalent interactions. We have demonstrated that there is a remarkable interplay between either anion– $\pi$  [17] or cation– $\pi$  interactions and either face-to-face aromatic or hydrogen bonding interactions in complexes where two kinds of non-covalent interactions coexist. This interplay can lead to strong cooperative effects, as has been recently demonstrated experimentally [18,19]. Moreover, we have also demonstrated synergistic effects between C–H/ $\pi$  and face-to-face  $\pi$ – $\pi$  interactions by means of *ab initio* calculations [20]. Fortunately, experimental evidence for such contacts could be obtained from the Protein Data Bank (PDB) [21]. Finally, we have demonstrated that the T-shaped binding properties of a variety of compounds containing nitrogen atoms in the aromatic ring is affected if these nitrogen atoms are participating in hydrogen bonding [22]. In the present report, we study how the T-shaped aromatic interaction between pyridine and benzene is influenced if the nitrogen atom of the pyridine participates in a variety of interactions/bonding associations ( $\sigma$  interactions). We have selected several pyridine moieties, i.e. **2–7** (Fig. 1, top), where the nitrogen atom in the structure is involved in: (i) either weak (**2**) or strong (**3**) hydrogen bonding interactions; (ii) it is protonated (**4**); (iii) it is methylated (methylpyridinium **5**); (iv) it is oxidized (**6**); and, finally, it is coordinated to a metal (Ag<sup>I</sup>, **7**). We have computed and compared the binding energies and geometries of the edge-to-face  $\pi$ – $\pi$  complexes **8–14** depicted in Fig. 1, bottom. We have used the Bader's theory of 'atoms-in-molecules' (AIM) [23], which has been widely used to characterize a great variety of interactions [24–26], to analyze the behaviour of the edge-to-face interaction in the complexes **8–14**. We have analyzed the differences in the nature of the T-shaped interaction in the complexes by means of the Molecular Interaction Potential with Polarization (MIPp) partition scheme [27], which has been successfully used to characterize a variety of non-covalent interactions [28,29].

<sup>\*</sup> Corresponding authors. Fax: +34 971 173426 (A. Frontera).  
E-mail address: [toni.frontera@uib.es](mailto:toni.frontera@uib.es) (A. Frontera).

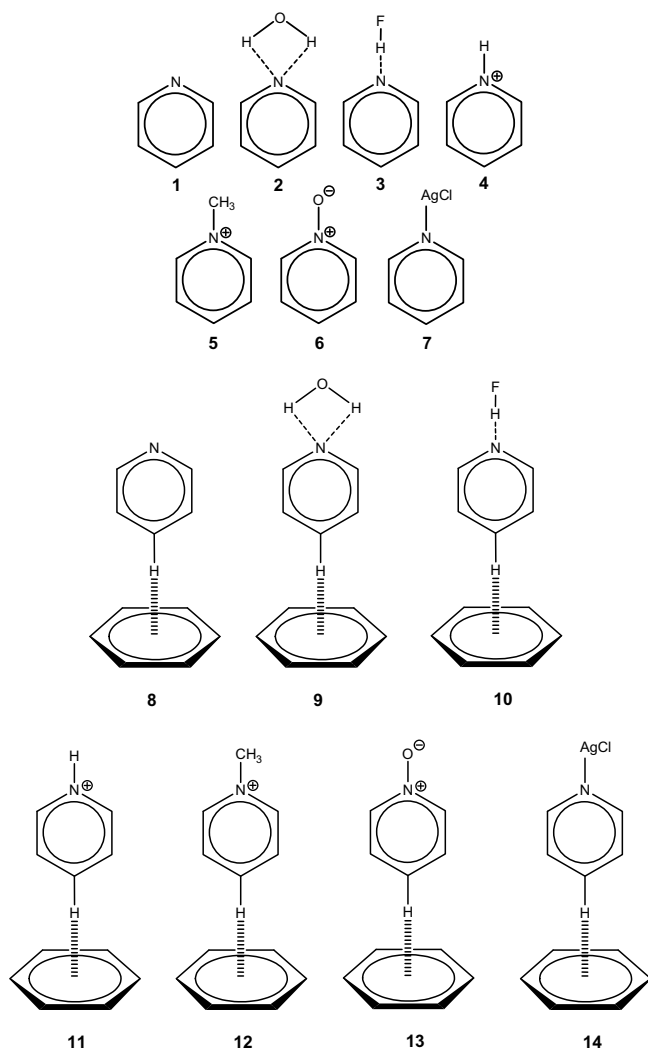


Fig. 1. Compounds 1–7 and complexes 8–14 studied in this work.

## 2. Computational methods

The geometries of all complexes studied in this work were fully optimized at the RI-MP2/TZVP level of theory using the Turbomole program [30–32]. These geometries were used to perform single point calculations using the augmented correlation-consistent polarized valence triple- $\zeta$  (aug-cc-pVTZ) basis set in order to obtain more accurate energetic values. For the silver atom the calculations were performed using a relativistic effective core potential (ECP28MWB) [33]. The binding energies were calculated with correction for the basis set superposition error (BSSE) by using the Boys–Bernardi counterpoise technique [34]. The optimization of the complexes has been performed imposing either  $C_s$  symmetry (complexes 12 and 19) or  $C_{2v}$  (rest of complexes). Other possible conformations of complexes have not been considered because the ultimate aim of this study is to verify the influence of the participation of the nitrogen atom of the pyridine ring in a variety of interactions/bonding associations upon the T-shaped non-covalent interactions. Therefore we have only concentrated on those complex geometries. A possible disadvantage of imposing symmetry is that highly nonsymmetrical conformations may often have similar or even higher binding energies compared to the more symmetric ones [35–37]. In spite of this possible drawback due to the imposed symmetry, it is likely that the trends of the results

discussed in this manuscript will remain valid. The number of imaginary frequencies (NImag) of all complexes has been included in the tables.

It is known that the MP2 level tends to overestimate the binding energy of the three main conformations of the benzene dimer compared to higher levels of theory [12,13]. It should be also mentioned that the T-shaped geometry is the conformation where the agreement between MP2 and CCSD(T)/aug-cc-pVQZ levels of theory is the best. Moreover, the main objective of this study is not to obtain the highest accuracy for each binding energy. Instead, it is, as aforementioned, to analyze the influence upon the T-shaped interaction provoked by the participation of the nitrogen atom of the pyridine ring in a variety of interactions and bonding.

The AIM analysis has been performed by means of the AIM2000 version 2.0 program [38] using the MP2/TZVP wavefunction. The physical nature of the non-covalent interactions has been studied using the Molecular Interaction Potential with polarization (MIPp) method [27]. The MIPp is a convenient tool for predicting binding properties. It has been successfully used for rationalizing molecular interactions such as hydrogen bonding and ion- $\pi$  interactions and for predicting molecular reactivity [28,29,16]. The MIPp partition scheme is an improved generalization of the MEP where three terms contribute to the interaction energy, (i) an electrostatic term identical to the MEP [39], (ii) a classical dispersion–repulsion term [40], and (iii) a polarization term derived from perturbational theory [41].

## 3. Results and discussion

### 3.1. Preliminary considerations

Before starting the computational study of the T-shaped complexes depicted in Fig. 1, bottom, we performed a search in the Cambridge Structural Database (CSD) with the purpose of studying the structural characteristics of edge-to-face complexes of pyridine and benzene. Crystal structures are rich in geometrical information and often reveal effects that have not been noticed by the original authors. The utility of crystallography and the CSD in analyzing geometrical parameters and non-covalent interactions is clearly established [42]. The search has been performed imposing several constraints: first, a hit was stored when six non-bonded contacts exist between the *para* aromatic hydrogen atom of the pyridine and the six carbon atoms of the aromatic ring. Second, to ensure the T-shaped geometry, we have constrained the angle between the pyridine and phenyl ring planes to range between 60 and 120 degrees. When analyzing the results, we observed that in all hits the nitrogen atom of the pyridine was not ‘naked’, instead, it was always participating either in bonding (covalent, ligand or non-covalent) or it was bearing a positive charge (protonated or alkylated). In Fig. 2, we show a selected representative example of each type of hit. In the first structure, CSD reference code MAFQIU [43], a quinoline molecule is participating in hydrogen bonding via the nitrogen atom and simultaneously the hydrogen atom is establishing an edge-to-face interaction with a phenol ring. We have found 22 structures in the CSD of this type. In the second structure (ZUTDAT) [44], a monoprotonated bispyridine is interacting through the *para* hydrogen atom of the protonated pyridine with a phenyl group of the counterion tetraphenylborate. We have found 23 structures in the CSD of T-shaped complexes of phenyl groups with charged pyridines. The third structure is characterized by the presence of a pyridine oxide moiety (NAMBUIZ) [45]. In this case the pyridine ring is forming two T-shaped interactions using both *ortho* and *para* hydrogen atoms. We have found only four structures involving pyridine oxide in the CSD. Lastly, in the fourth structure a transition metal (Ag) is coordinated by the nitrogen

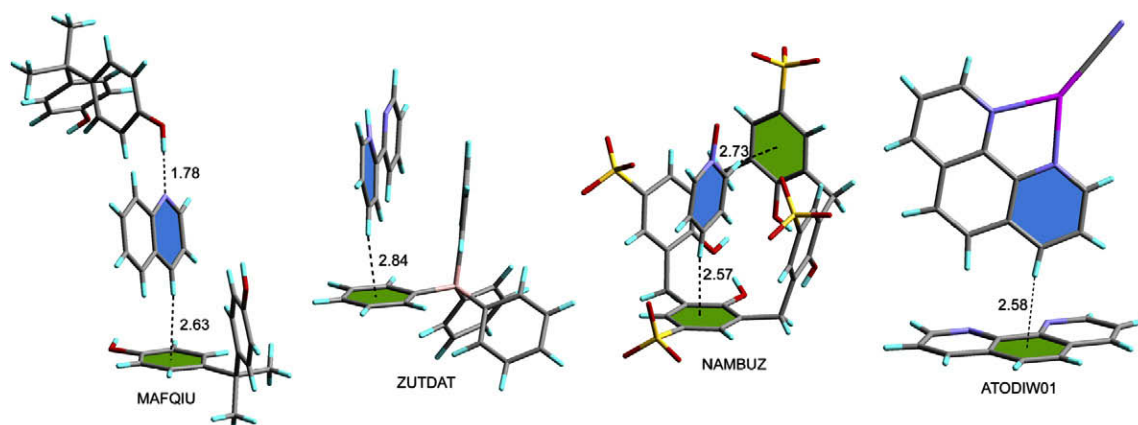


**Fig. 2.** Solid state structures (partial views) of several compounds exhibiting T-shaped interactions, see text for details. Pyridine rings are illustrated in blue and phenyl rings in green. Distance units are Å. (For interpretation of the references to colour in this figure legend, the reader is referred to the web version of this article.)

atom of a pyridine ring (ATODIW01 [46]). This type of structures is the most abundant in the CSD, we have found 123 hits for the search of T-shaped complexes where the nitrogen atom of the pyridine is coordinated to a transition metal, and there is a great variety of metals in the retrieved structures.

### 3.2. Geometric and energetic results

In Table 1 we summarize the binding energies without and with the basis set superposition error (BSSE) correction ( $E$  and  $E_{\text{BSSE}}$ , respectively) and equilibrium distances ( $R_e$ ) of complexes **8–14** at the RI-MP2/aug-cc-pVTZ//RI-MP2/TZVP level of theory. From the inspection of the results several interesting points arise. First, the T-shaped interaction of pyridine with benzene (BEN) is more favourable than the BEN-BEN interaction at the same level [12,13] (3.37 kcal/mol). Second, the binding energy of complexes **9–14** is more negative than **8**. The T-shaped interaction is reinforced in complexes **11** and **12**, where nitrogen atom of pyridine is positively charged. This enhancement is very modest in the pyridine oxide (complex **13**). It is also very modest in complexes **9** and **10**, where the nitrogen atom of the pyridine is participating in hydrogen bonding. Third, the enhancement is almost 1 kcal/mol when the nitrogen atom is coordinated to Ag(I). This result is important, since there are a great number of structures of nitrogen-containing aromatics that are used in coordination chemistry, and this interaction can have an important influence on either the crystal packing of these molecules or their interaction with other molecules via T-shaped non-covalent bonding. It is also in agreement with the important number of hits obtained from the CSD for this type of systems. Fourth, the enhancement is very important in charged pyridines, complexes **11** and **12**, due to the increment in

the acidity of the hydrogen atom that interacts with the  $\pi$ -cloud of BEN due to the positive charge. Finally, the equilibrium distances ( $R_e$ ) of complexes **9–14** are shorter than the  $R_e$  of complex **8** in agreement with the interaction energies. The shortening in charged complexes **11** and **12** is very significant (greater than 0.15 Å).

To further study the effect of several  $\sigma$  interactions via the nitrogen atom upon the T-shaped  $\pi$  interaction, we have also calculated the complexes present in Fig. 3. We have not found any crystallographic evidence of this type of complexes because of the reduced number of perfluorophenyl derivatives in the CSD. In these complexes the pyridine moieties are the same than the previously studied where the *para* hydrogen atom has been substituted by a fluorine atom. In addition, the benzene ring has been substituted by the electron deficient hexafluorobenzene (HFB) ring. Therefore, in these complexes the  $\pi$  interaction can be defined as a lone pair ( $\text{lp}$ )/ $\pi$  interaction. The geometric and energetic results are summarized in Table 2. It can be observed that the  $\text{lp}/\pi$

**Table 1**

Interaction energies with and without BSSE correction ( $E$  and  $E_{\text{BSSE}}$ , respectively) in kcal/mol, number of imaginary frequencies (NImag) and equilibrium distances ( $R_e$ , Å) computed at the RI-MP2/aug-cc-pVTZ//RI-MP2/TZVP level of theory for complexes **8–14**.

Complex	$E$	$E_{\text{BSSE}}$	NImag	$R_e$
<b>8</b>	−5.46	−4.02	0	2.295
<b>9</b>	−5.75 <sup>a</sup>	−4.25 <sup>a</sup>	1	2.275
<b>10</b>	−6.05 <sup>a</sup>	−4.53 <sup>a</sup>	0	2.253
<b>11</b>	−11.48	−9.79	0	2.123
<b>12</b>	−10.97	−9.31	0	2.134
<b>13</b>	−5.58	−4.06	0	2.258
<b>14</b>	−6.77	−4.92	2	2.232

<sup>a</sup> Computed as binary (not ternary) systems, i.e. **2** + BEN → **9** and **3** + BEN → **10**.

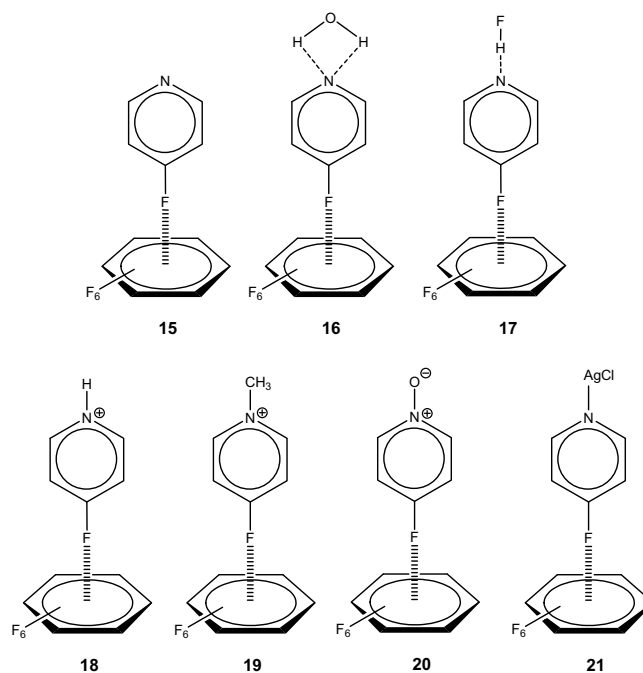


**Fig. 3.** Complexes **15–21**.

**Table 2**

Interaction energies with and without BSSE correction ( $E$  and  $E_{\text{BSSE}}$ , respectively in kcal/mol), number of imaginary frequencies (NImag) and equilibrium distances ( $R_e$ , Å) computed at the RI-MP2/aug-cc-pVTZ//RI-MP2/TZVP level of theory for complexes **15**–**21**.

Complex	$E$	$E_{\text{BSSE}}$	NImag	$R_e$
<b>15</b>	−3.61	−2.31	0	2.876
<b>16</b>	−3.46 <sup>a</sup>	−2.57 <sup>a</sup>	1	2.859
<b>17</b>	−3.26 <sup>a</sup>	−1.95 <sup>a</sup>	0	2.871
<b>18</b>	−1.68	−0.47	0	2.976
<b>19</b>	−1.77	−0.53	0	2.959
<b>20</b>	−3.58	−2.23	0	2.854
<b>21</b>	−3.08	−1.59	2	2.889

<sup>a</sup> Computed as binary (not ternary) systems, i.e. **2**<sub>F</sub> + HFB → **16** and **3**<sub>F</sub> + HFB → **17**.

interaction is energetically less favourable than the T-shaped aromatic interaction. The results of Table 2 indicate that the effect of covalent/non-covalent bonding of the pyridine via the nitrogen atom on the strength of the lp/ $\pi$  interaction is diverse. In the hydrogen bonded complexes **16** and **17** and in the pyridine oxide **20**, the effect is almost negligible. In contrast, in charged complexes **18** and **19** the lp/ $\pi$  interaction is considerably weakened, indicating that the lp of the fluorine atom is conjugated with the  $\pi$ -system to stabilize the positive charge. Thus, it is less available to interact with the electron deficient HFB. The same argument is applicable to complex **21**, where the lp of the fluorine atom is conjugated along the  $\pi$ -system in order to compensate the potent electron withdrawing effect of the silver atom coordinated to the nitrogen atom.

### 3.3. AIM results

The AIM analysis is summarized in Table 3 and it gives some helpful information regarding the strength of the non-covalent interactions involved in complexes **8**–**21**. It has been demonstrated that the value of the electron charge density at the critical points (CP) that are generated in  $\pi$ – $\pi$  and H-bonded complexes can be used [47] as a measure of the bond order or Electronic Sharing Index (ESI) [48]. For describing interactions involving aromatic rings, the values of the electron charge density at the cage CPs have been found very useful [16,17,10]. In Fig. 4 we show the distribution of CPs in complexes **8** and **15** as representative examples of complexes **8**–**14** and **15**–**21**, respectively. In all complexes, several

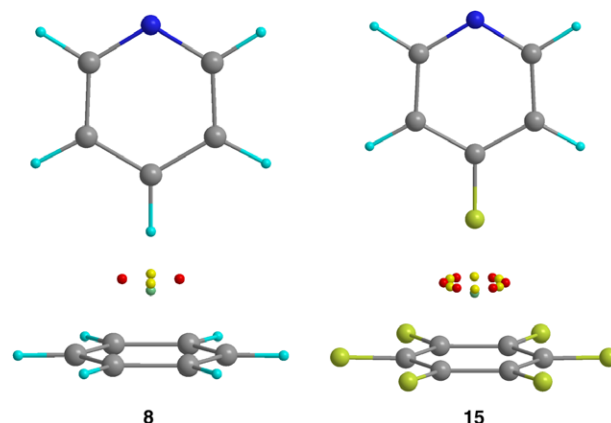


**Fig. 4.** Distribution of critical points (CP) in complexes **8** and **15**. Bond CPs are depicted in red, ring CPs in yellow and cage CPs in green. (For interpretation of the references to colour in this figure legend, the reader is referred to the web version of this article.)

bond CPs, several ring CPs and one cage CP describe the edge-to-face interaction. The number of bond and ring CPs depends upon the symmetry and the nature of the complex. That is, for complexes **8**–**10**, two bond and two ring CPs are obtained. For complexes **11** and **13**, four bond and four ring CPs are obtained. For complex **12** only one bond and one ring CPs are obtained. Finally, for the rest of complexes (**14**–**21**), six bond and six ring CPs are obtained. The bond CPs connect the hydrogen/fluorine atom with carbon atoms of the ring and the ring CPs connect the hydrogen/fluorine atom with the middle of C–C bonds. The cage CP connects the hydrogen/fluorine atom to the center of the aromatic ring.

In Table 3 we show the values of the electron charge density ( $\rho$ ) and its Laplacian ( $\nabla^2\rho$ ) computed at the cage critical point that characterizes the T-shaped interaction. We have chosen the cage CP because a common feature of all complexes is the presence of one cage CP describing the T-shaped interaction. A previous study has shown the utility of this property in describing this type of non-covalent bonding [22]. We also summarize the variation of the  $\rho$  value in the complexes **9**–**14** with respect to the complex **8** (naked nitrogen atom). These values give information about the interplay between the T-shaped non-covalent interaction involved in the complexes and the participation of the nitrogen atom in several bonding modes. The values obtained for the Laplacian are in all cases positive, as is common in closed-shell interactions. First, it is worth mentioning that the value of the charge density computed at the cage CPs is greater in complexes **9**–**14** than in complex **8**, in agreement with the interaction energies and confirming that there is a strengthening of the T-shaped interaction in these complexes. Second, the value of the charge density computed at the cage CPs is smaller in complexes **18**, **19** and **21**, than in complex **15**, in agreement with the interaction energies and with the lengthening of equilibrium distances, indicating that the T-shaped interaction weakens in these complexes. In addition, the charge density computed at the cage CPs is larger in complex **16** than in complex **15**, in agreement with the interaction energy and with the shortening of the equilibrium distance, indicating that the T-shaped interaction strengthens in this complex. An anomalous behaviour is found in complexes **17** and **20**. In both complexes the charge density computed at the cage CPs is larger than the one obtained for complex **15**, in disagreement with the interaction energies and in agreement with the shortening of equilibrium distances. A likely explanation for this disagreement is that the binding energies are computed at a different level of theory than the geometries. This issue can specially affect complexes **16**–**17** and **20** because they

**Table 3**

Electron charge density ( $\rho$ , a.u.) and its Laplacian ( $\nabla^2\rho$ , a.u.), computed at the cage critical points (RI-MP2/TZVP) for complexes **8**–**21** and the variation of the charge density ( $\Delta\rho$ ) and the equilibrium distance ( $\Delta R_e$ ) of complexes **9**–**14** and **16**–**21** with respect to **8** and **15**, respectively.

Complex	$10^2 \times \rho$	$10 \times \nabla^2\rho$	$10^3 \times \Delta\rho$	$\Delta R_e$
<b>Benzene complexes</b>				
<b>8</b>	0.6592	0.3376	0.0000	0.000
<b>9</b>	0.6788	0.3480	0.1956	−0.020
<b>10</b>	0.7011	0.3602	0.4188	−0.042
<b>11</b>	0.8404	0.4328	1.8123	−0.172
<b>12</b>	0.8270	0.4255	1.6775	−0.161
<b>13</b>	0.6941	0.3569	0.3488	−0.037
<b>14</b>	0.7218	0.3703	0.6259	−0.063
<b>Hexafluorobenzene complexes</b>				
<b>15</b>	0.3695	0.2534	0.0000	0.000
<b>16</b>	0.3792	0.2608	0.0965	−0.017
<b>17</b>	0.3710	0.2547	0.0147	−0.005
<b>18</b>	0.3073	0.2062	−0.6225	0.100
<b>19</b>	0.3169	0.2134	−0.5263	0.083
<b>20</b>	0.3829	0.2635	0.1334	−0.022
<b>21</b>	0.3594	0.2458	−0.1016	0.013



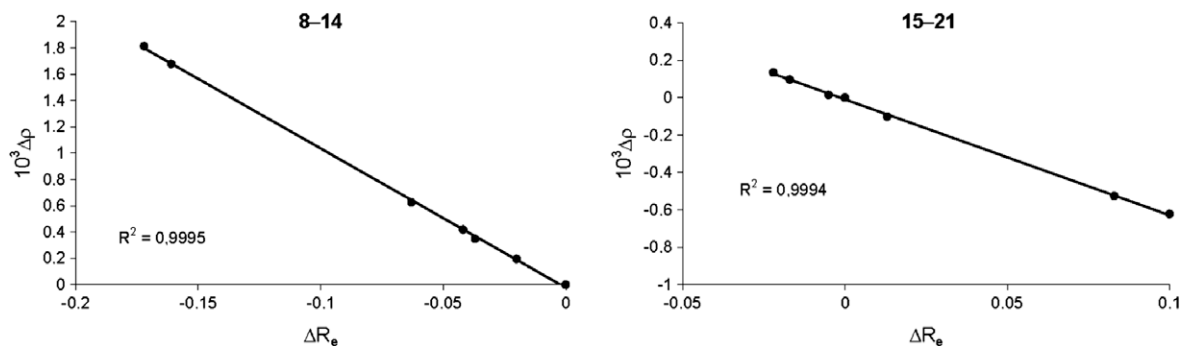


Fig. 5. Regression plots between the charge density  $\Delta\rho$  ( $\times 10^3$ ) at the cage critical point (in a.u.) and the equilibrium distances  $\Delta R_e$  (Å) of the T-shaped complexes **8–14** (left) and complexes **15–21** (right).

have very similar binding energies and equilibrium distances compared to **15**.

For each series of complexes (**8–14** and **15–21**) the binding energy correlates with the values of  $\rho$  at the cage CP (see Table 3). We have found interesting and strong ( $R^2 = 0.9995$  and  $R^2 = 0.9994$ ) relationships between the charge density at the cage CP and the relative equilibrium distances ( $\Delta R_e$ , see Table 3) of the complexes for each series (see Fig. 5). These relationships indicate that the value of the charge density at the cage CP can be used as a measure of ESI in the T-shaped interactions. These linear correlations are probably due to the small range of distances present in these complexes. An exponential relationship is expected in a large range of distances [49].

### 3.4. MIPp analysis

We have used the MIPp partition scheme to analyze the physical nature of the T-shaped interaction involved in the complexes. MIPp partition scheme is also a helpful tool for understanding the bonding mechanism and to rationalize the interaction energies of the T-shaped interaction in the absence (**1**) and presence (**2–6**) of  $\sigma$ -interaction (see Table 4). The MIPp calculation has not been performed for compound **7** because the silver atom is not parameterized. In all compounds, the total interaction energy ( $E_t$ ) is basically dominated by electrostatic effects ( $E_e$ ), since the polarization ( $E_p$ ) and dispersion–repulsion contributions ( $E_{vw}$ ) are very small. In compounds **2**, **3** and **5** the  $E_e$  term becomes more negative and the  $E_p$  term remains almost constant, in comparison to compound **1** indicating that the enhancement of the T-shaped interaction when the pyridine is either establishing hydrogen bonding interactions (compounds **2** and **3**) or it is oxidized (compound **5**) is due to electrostatic effects. In compounds **4** and **5**, there is an important increment in the  $E_e$  term because these compounds are positively charged. These results are in agreement with the binding energies reported in Table 1. Finally, for all compounds **2–5** the  $E_{vw}$  term becomes positive, compared to **1**. This is because the MIPp minimum

gets closer to the aromatic ring, provoking an increase of the van der Waals repulsion term.

### 4. Concluding remarks

In summary, the results reported in this manuscript stress the importance of non-covalent interactions involving aromatic systems. We have demonstrated that the T-shaped aromatic interaction between pyridine and benzene can be modulated by using  $\sigma$ -interactions via the nitrogen atom of the pyridine ring. We have found in the CSD many examples that illustrate this issue for complexes **9–14**. Due to the presence of a great number of aromatic rings containing heteroatoms in biological systems, this effect can be important and might help to understand some biological processes where the interplay between both interactions exist. It also should be taken into account in supramolecular chemistry and crystal engineering fields.

### Acknowledgments

We thank the DGICYT and Govern Balear of Spain (projects CTQ2005-08989-01 and PCTIB-2005GC3-08, respectively) for financial support. We thank the CESCA for computational facilities.

### References

- [1] E.A. Meyer, R.K. Castellano, F. Diederich, *Angew. Chem. Int. Ed.* 42 (2003) 1210.
- [2] S.K. Burley, G.A. Petsko, *Science* 229 (1985) 23.
- [3] C.A. Hunter, J.K.M. Sanders, *J. Am. Chem. Soc.* 112 (1990) 5525.
- [4] P. Chakrabarti, U. Samanta, *J. Mol. Biol.* 251 (1995) 9.
- [5] U. Samanta, P. Chakrabarti, *Protein Eng.* 14 (2001) 7.
- [6] M. Macias, S. Wiesner, M. Sudol, *FEBS Lett.* 513 (2002) 30.
- [7] R. Chelli, F.L. Gervasio, P. Procacci, V. Schettino, *J. Am. Chem. Soc.* 124 (2002) 6133.
- [8] R. Meurisse, R. Brausseau, A. Thomas, *Biochim. Biophys. Acta* 1649 (2003) 86.
- [9] J.B. Mitchell, C.L. Nandi, I.K. McDonald, J.M. Thornton, S.L. Price, *J. Mol. Biol.* 239 (1994) 315.
- [10] E. Cauët, M. Rooman, R. Wintjens, J. Liévin, C. Biot, *J. Chem. Theor. Comput.* 1 (2005) 472.
- [11] K. Vanommeslaeghe, P. Mignon, S. Loverix, D. Tourwé, P.J. Geerlings, *J. Chem. Theor. Comput.* 2 (2006) 1444.
- [12] M.O. Sinnokrot, C.D. Sherrill, *J. Phys. Chem. A* 107 (41) (2003) 8377.
- [13] T. Janowski, P. Pulay, *Chem. Phys. Lett.* 447 (2007) 27.
- [14] A. Garcia-Raso et al., *Inorg. Chem.* 46 (2007) 10724.
- [15] A. Frontera, D. Quiñero, A. Costa, P. Ballester, P.M. Deyà, *New J. Chem.* 31 (2007) 556.
- [16] D. Quiñero et al., *ChemPhysChem* 7 (2006) 2487.
- [17] D. Quiñero et al., *Angew. Chem. Int. Ed.* 41 (2002) 3389.
- [18] L.A. Barrios et al., *Inorg. Chem.* 47 (2008) 5873.
- [19] M. Zaccachedu, C. Filippi, F. Buda, *J. Phys. Chem. A* 112 (2008) 1627.
- [20] D. Quiñero et al., *Theor. Chem. Acc.* 120 (2008) 385.
- [21] F.C. Bernstein et al., *J. Mol. Biol.* 112 (1977) 535.
- [22] D. Escudero, A. Frontera, D. Quiñero, P.M. Deyà, *J. Phys. Chem. A* 112 (2008) 6017.
- [23] R.F.W. Bader, *Chem. Rev.* 91 (1991) 893.
- [24] J.R. Cheeseman, M.T. Carroll, R.F.W. Bader, *Chem. Phys. Lett.* 143 (1998) 450.

Table 4

Contributions to the total ( $E_t$ ) interaction energy (kcal/mol) computed using MIPp of compounds **1–6** with  $C^{4-}$  at the minimum along the line defined by the ideal interacting trajectory for a T-shaped interaction at the HF/6-311++G\*\*//RI-MP2/TZVP level of theory.

Compound	$E_e$	$E_p$	$E_{vw}$	$E_t$
<b>1</b>	−2.03	−0.28	−0.21	−2.52
<b>2</b>	−2.93	−0.25	0.12	−3.05
<b>3</b>	−3.45	−0.25	0.12	−3.58
<b>4</b>	−17.10	−0.23	0.11	−17.23
<b>5</b>	−16.63	−0.24	0.13	−16.74
<b>6</b>	−3.15	−0.27	0.12	−3.29

- [25] U. Koch, P.L.A. Popelier, *J. Phys. Chem.* 99 (1995) 9794.
- [26] F.J. Luque, J.M. Lopez, M.L. de la Paz, C. Vicent, M. Orozco, *J. Phys. Chem. A* 102 (1998) 6690.
- [27] F.J. Luque, M. Orozco, *J. Comput. Chem.* 19 (1998) 866.
- [28] B. Hernández, M. Orozco, F.J. Luque, *J. Comput-Aided Mol. Des.* 11 (1997) 153.
- [29] F.J. Luque, M. Orozco, *J. Chem. Soc. Perkin Trans. 2* (1993) 683.
- [30] R. Ahlrichs, M. Bär, M. Hacer, H. Horn, C. Kömel, *Chem. Phys. Lett.* 162 (1989) 165.
- [31] M.W. Feyereisen, G. Fitzgerald, A. Komornicki, *Chem. Phys. Lett.* 208 (1993) 359.
- [32] O. Vahtras, J. Almlöf, M.W. Feyereisen, *Chem. Phys. Lett.* 213 (1993) 514.
- [33] A. Niklass, M. Dolg, H. Stoll, H. Preuss, *J. Chem. Phys.* 102 (1995) 8942.
- [34] S.B. Boys, F. Bernardi, *Mol. Phys.* 19 (1970) 553.
- [35] O.B. Berryman, V.S. Bryantsev, D.P. Stay, D.W. Johnson, B.P. Hay, *J. Am. Chem. Soc.* 129 (2007) 48.
- [36] P.U. Maheswari et al., *Inorg. Chem.* 45 (2006) 6637.
- [37] M.M.G. Antonisse, B.H.M. Snellink-Ruel, I. Yigit, J.F.J. Engbersen, D.N. Reinhoudt, *J. Org. Chem.* 62 (1997) 9034.
- [38] F. Biegler-König, J. Schönbohm, D. Bayles, *J. Comp. Chem.* 22 (2001) 545.
- [39] E. Scrocco, J. Tomasi, *Top. Curr. Chem.* 42 (1973) 95.
- [40] M. Orozco, F.J. Luque, *J. Comput. Chem.* 14 (1993) 587.
- [41] M.M. Francl, *J. Phys. Chem.* 89 (1985) 428.
- [42] A. Nangia, K. Biradha, G.R. Desiraju, *J. Chem. Soc. Perkin Trans. 2* (1996) 943.
- [43] B. Hatano, A. Alkawa, H. Tagaya, H. Takahashi, *Chem. Lett.* 33 (2004) 1276.
- [44] P.K. Bakshi, T.S. Cameron, O. Knop, *Can. J. Chem.* 74 (1996) 201.
- [45] B.-T. Zhao, H. Wang, H.-Y. Zhang, Y. Liu, *J. Mol. Struct.* 740 (2005) 101.
- [46] G.A. Bowmaker, P.C. Effendy, B.W. Junk, A.H. Skelton, Z. White, *Naturforsch. B: Chem. Sci.* 59 (2004) 1277.
- [47] A. Frontera et al., *J. Phys. Chem. A* 110 (2006) 9307.
- [48] R.L. Fulton, S.T. Mixon, *J. Phys. Chem.* 97 (1993) 7530.
- [49] E. Espinosa, I. Alkorta, J. Elguero, E. Molins, *J. Chem. Phys.* 117 (2002) 5529.